Spring 3-25-2022

Analyzing Inhibitors of the SARS-CoV-2 Endoribonuclease nsp15

Mary Staunton
mary.staunton@uconn.edu

Analyzing Inhibitors of the SARS-CoV-2 Endoribonuclease nsp15

Mary Staunton

Honors Thesis, Biological Sciences

Thesis Advisor/Honors Advisor: Dr. James Cole, Department of Molecular and Cell Biology, University of Connecticut

---

May 2022

Abstract

The global pandemic caused by the virus SARS-CoV-2 has devastated the world. A flurry of research into the structures and activities of the virus have identified several viable targets for drug therapy, including the endoribonuclease nsp15, also known as EndoU. EndoU has been shown to play a role in diminishing the host cell's immune response to the virus by cleaving signaling dsRNA, specifically targeting uridine sequences. The development of the crystal structure nsp15 allowed our lab along with others to perform virtual screenings to identify inhibitors that might be able to dock at the active site and inhibit the activity of the enzyme. Potential inhibitors were screened through a FRET-based enzyme assay and hits were then titrated to examine potency of the inhibitor. Although no new hits for inhibitors were identified, I was able to characterize some known inhibitors and the effect that a divalent ion has on the inhibition of the enzyme. For all of our identified inhibitors, there is increased effectiveness when the reaction is done in the presence of Mn^{2+} rather than Mg^{2+}. Further research into the binding of the divalent ion and the active site of the enzyme is needed to further characterize the role of the divalent ion cofactor and to find better inhibitors that could be used as drug therapy treatments of COVID-19.

1. Introduction

In December 2019, the first human cases of COVID-19 were reported in Wuhan City, China (1). Since then, the virus has evolved into a global pandemic that has devastated the world. As of September 2021, there have been over 200 million confirmed cases of COVID-19, including nearly 5 million deaths (2). COVID-19 is a respiratory disease caused by the coronavirus SARS-CoV-2, which is in the same family as the SARS-CoV and MERS-CoV viruses which caused pandemics in 2003 and 2012, respectively (1). It has been difficult to effectively prevent the transmission of this virus among the human population, but the development of vaccines was an incredibly successful development. However, as the virus mutates and vaccines become less effective, there still remains a need for additional drug therapies. The main treatment currently in use is a drug called remdesivir, which has shown limited success in treating the active infections (3). Another promising drug is molnupiravir, an oral treatment developed by Merck that has yet to receive emergency approval (13). The dire need for more effective treatments has led to a flurry of interest in the basic virology of SARS-CoV-2 and possible targets for new drug therapies.

The SARS-CoV-2 virus is a positive-sense RNA with 16 nsps (non-structural proteins) (4). Several of the nsps compose the replication and transcription complex (RTC) which performs RNA synthesis (4). An atomistic model of the RTC shows a hexameric superstructure of proteins assembled around a central protein, nsp15, and identified several roles of this complex which include proofreading, template switching, mRNA capping, and hydrolysis of double-stranded RNA (dsRNA) (16). The protein of interest for this study is nsp15, an endoribonuclease also known as EndoU (6). Nsp15 is highly conserved across all coronaviruses, with the SARS-CoV-2 protein sharing 88% sequence identity and 95% similarity with the

SARS-CoV homolog, and much stronger than its arterivirus ortholog nsp11 (5). The similarity of the nsp15 sequences among different coronaviruses suggests that an inhibitor of the SARS-CoV-2 enzyme will work against other emerging coronaviruses (6).

The nsp15 protein was originally thought to be essential for replication, but the Baker lab demonstrated that EndoU-deficient coronaviruses replicated with only a subtle change from normal rates in fibroblast cells (6). The nsp15 enzyme was first identified as an IFN (interferon) antagonist of SARS-CoV by screening using an alphavirus replication-defective vector (VRP) (14). To further study the activity of nsp15, cells were infected with a virus containing a nsp15 mutant with alanine substitution at its histidine active site, and EndoU activity was inactivated (7). This resulted in limited reproduction of the virus and rapid cell death which helped to identify nsp15 as a major antagonist to the type 1 interferon (IFN) antiviral pathway (7). The Deng and Kindler labs then discovered that multiple dsRNA sensing pathways are independently activated to inhibit viral replication in cells infected with EndoU-deficient CoVs (6,8). For example, EndoU was shown to be a direct antagonist to the IFN pathway as a catalytically inactive mutant of nsp15 allowed for the detection of viral dsRNA by the MDA5 receptor, which initiated a robust type 1-IFN response and greatly reduced viral replication (7,8). Additional immune pathways at work in the presence of the inactive EndoU include PKR, which inhibits host and viral mRNA translation, and the OAS-RNase L pathway (6,8). These discoveries led researchers to believe that EndoU mediates evasion of the innate immunity pathway by cleaving viral dsRNA so that it is not detected (7,8).

The next step in understanding nsp15 was to identify the dsRNA target of EndoU. It was discovered that EndoU activity reduces the abundance of negative-sense RNA that contains polyU extensions with >12 uridines, a sequence that was identified as a pathogen associated

molecular pattern (PAMP) (9). When this sequence is cut by EndoU, the virus is able to evade detection by MDA5 and diminish the IFN response, allowing for increased viral replication (9). Further investigation into the specificity of nsp15 identified the critical residues as S294 and N278, which interact to select for uridine (15).

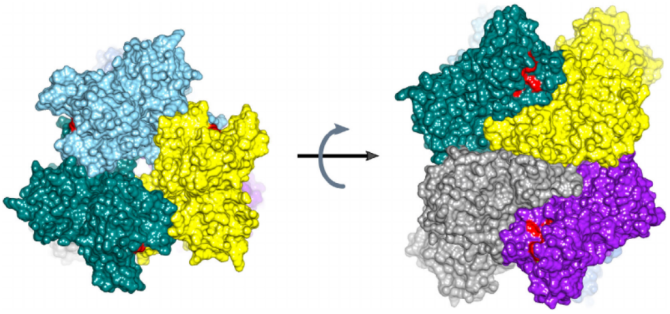

Figure 1.1: The surface of the SARS-CoV-2 EndoU hexamer with each subunit a different color and the active sites in red (from reference (5))

In 2020, a crystal structure of the SARS-CoV-2 EndoU protein was reported by the Kim lab (Figure 1.1). Researchers were able to identify the active site of the hexameric protein, which is located in a shallow groove between two β-sheets (5). This site has six main residues which are conserved across most CoVs, including His235, His250, Lys290, Thr341, Tyr343, and Ser294 (Figure 1.2). It was also reported that EndoU activity was dependent on the presence of a divalent metal ion, preferentially Mn^{2+} (5). The active site of nsp15 has a similar architecture to the eukaryotic metal-independent protein RNase A, despite having a completely different overall fold (17).

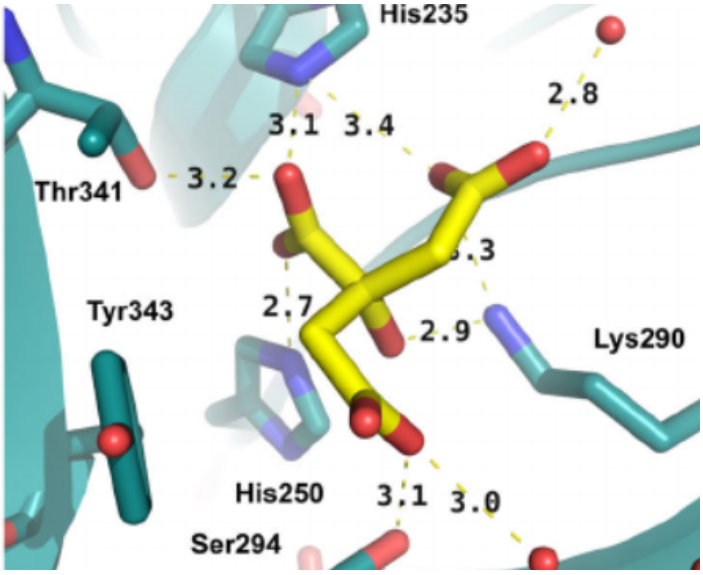

Figure 1.2: Binding of citrate to the six active site residues of SARS-CoV-2 nsp15.(From reference (5))

The hope to use nsp15 as a target gene for drug therapy lies in finding an inhibitor that can block the activity of EndoU. One study found an inhibitor, NSC95397, that did inhibit nsp15 enzymatic activity *in vitro* but did not inhibit viral replication when tested in VERO E6 cells (10). Another study identified an inhibitor, a 1,2,3-triazolo-fused betulonic acid derivative, which effectively inhibited nsp15 in another genus of coronaviruses called HCoV-229E and ultimately resulted in the inhibition of viral replication; unfortunately, this inhibitor did not exhibit the same effectiveness on the SARS-CoV-2 enzyme (11). Clearly there remains a need for further study to identify an inhibitor that can both inhibit the EndoU of SARS-CoV-2, function in live cells at an effective concentration, and meet all the other requirements for an antiviral treatment.

2. Materials & Methods

2.1 Materials

In this study, we sought to identify and characterize inhibitors of nsp15 using a FRET-based enzyme assay. This assay was modeled after previous studies on inhibition of SARS-CoV-2 nsp15, with modifications (5). The substrate used is a short oligonucleotide with the sequence 5′-56-FAM-dAr**U**dAdA-3TAMRA_N-3′ synthesized by Integrated DNA Technologies, containing the FAM fluorescent donor at the 5' terminus as well as a fluorescence quencher molecule, TAMRA, at the 3' end. The substrate will be cleaved at the single uracil residue (bolded and underlined) which will increase the fluorescent emission of FAM due to the separation of the FAM- and TAMRA molecules. To express EndoU in our lab, we transformed BL21 *E. Coli* with the plasmid pMCSG53 (reference 5) and the nsp15 protein was expressed and then purified using metal ion affinity and gel filtration chromatography by Dr. Cole.

2.2 Experimental Methods

EndoU Activity Assay

The reaction buffer contained 50 mM HEPES, pH 7.5, 50 mM KCl, and either 5 mM $MnCl_2$ or 10 mM $MgCl_2$. Inhibitors were dissolved in DMSO. Either Mg^{2+} or Mn^{2+} buffer and inhibitor compounds were combined into wells on a 96 well plate with 2-3 replicates of each inhibitor. EndoU was added and allowed to incubate for five minutes before adding substrate. Because the buffer used to dilute the enzyme and substrate lacked a divalent ion, the final concentration of divalent ion in the experimental well is 70% less than that of the control wells with only buffer. The assay was run at 200 nM substrate, 100 nM enzyme, 20 μM inhibitor and 100 μL total volume. We included several control wells that lacked inhibitor to use as a reference. Immediately after adding the substrate, the plate was read on a SpectraMax i3x fluorescence

plate reader to monitor product formation. The fluorescence emission was recorded at room temperature for 10 minutes using the minimum point spacing, typically 11 seconds. The data were reduced to produce Vmax slopes for the first five minutes of the reaction. The amount of inhibition was calculated as a percentage based on the average slope of each inhibitor compared to the controls (Equation 1.1). Any compounds shown to significantly inhibit EndoU activity and reduce fluorescence were then titrated in a separate assay to evaluate their potency as an inhibitor.

$$(1.1) \qquad Percent\ Inhibition = \left(1 - \frac{average\ Vmax\ of\ inhibited\ enzyme}{average\ Vmax\ of\ control}\right) \times 100$$

I determined the potency of each inhibitor by calculating the IC_{50} values, or the concentration of the inhibitor needed to reduce the activity of the enzyme by half. To find this value, I calculated the percent inhibition for each concentration of inhibitor from the titration assays and plotted them using the Kaleidagraph program. The data were fit to Equation 1.2, where I_0 is the % inhibition in the absence of inhibitor and ΔI is the maximal % inhibition. In these fits, I_0, ΔI, and IC_{50} were all treated as adjustable parameters. The IC_{50} value was given as the parameter m3, which corresponds to the concentration at the inhibitor that gives half-maximal inhibition. We were also able to evaluate the reliability of the fitted parameters with an error estimate as well as an R value.

$$(1.2) \qquad Percent\ Inhibition = I_0 + \left(\Delta I \times \frac{[Inhibitor]}{[Inhibitor] + IC_{50}}\right)$$

Identification of Potential Inhibitors

To identify potential inhibitors to test in our study, we used two approaches based on a published crystal structure of EndoU (Figure 2.1); virtual screening and an artificial intelligence algorithm developed by Atomwise, Inc. For virtual screening, the GLIDE software package (Halgren, T. A. *et al.* Glide: a new approach for rapid, accurate docking and scoring. 2. Enrichment factors in

database screening. *Journal of Medicinal Chemistry* **47**, 1750–1759 (2004).) was used to screen libraries of commercially available compounds from companies including Chembridge, Life Chemicals, Enamine, and others that could potentially inhibit EndoU activity based on how well the compound fits into the active site of EndoU. This algorithm provided us with GLIDE scores to judge how well each compound docked at the EndoU active site and could be used as a predictor of effectiveness. Atomwise provided a library of 96 potential inhibitors; Dr. Cole screened them and identified four inhibitors, named UCA-1, UCA-2, UCA-3, and UCA-4 with IC_{50} values of 3.3, 4.8, 6.1, and 15.1 μM, respectively. We also chose inhibitors based on effectiveness in other studies. One study on the SARS-CoV nsp15 found several compounds that acted as inhibitors, including benzopurpurin B and congo red (18).

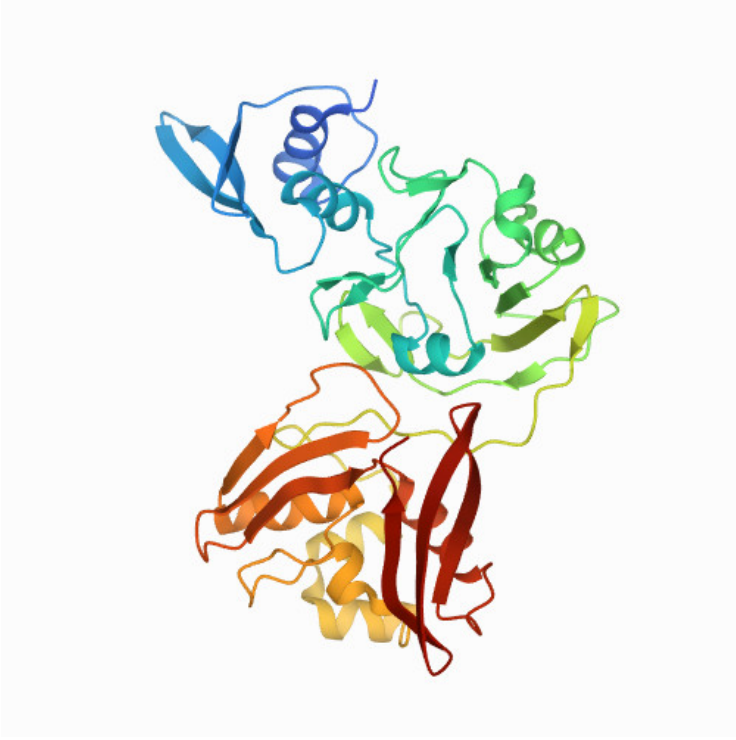

Figure 2.1: Crystal structure of nsp15 from SARS-CoV-2 generated by the Kim Lab (from reference (5)) and obtained from the Protein Data Bank (from reference (19)).

3. Results

3. 1 Screening of Enamine Compounds

Our ID number	Structure	Assay 1	Assay 2	IC50 (µM)	Glide Score
	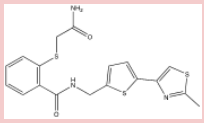	89	71	73.0	-5.917
UCA-1	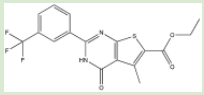	87	89	3.3	-4.622
UCA-3	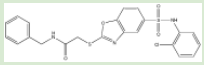	93	94	6.1	-4.870
	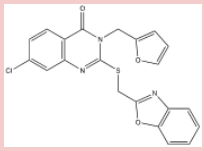	12	80	> 100	-4.716
UCA-4	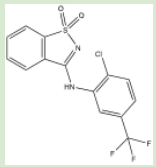	88	98	15.1	-4.876
UCA-2	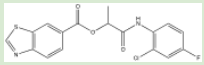	98	92	4.8	-5.042

Table 3.1: Compounds from Atomwise screened and titrated by Dr. Cole. Assay values represent percent inhibition of the compounds. Compounds highlighted in green had lower IC_{50} values and were investigated further as possible inhibitors. Compounds in red had IC_{50} values determined to be too high.

Dr. Cole used the SARS-CoV-2 nsp15 crystal structure generated by the Joachimiak lab (PDB 6VWW (19)) to screen for compounds with low GLIDE scores which would indicate high free binding energy and potent inhibition. Table 3.1 shows compounds from Atomwise that were inhibited EndoU in two initial assays at 100 μM . Dr. Cole then experimentally tested the top-scoring compounds to determine which ones actually inhibited nsp15. Active compounds were then titrated to determine IC_{50} values indicated above. Similarly, Dr. Cole titrated compounds identified using GLIDE that showed inhibition of EndoU in initial assays. The compounds with IC_{50} values of less than 50 μM were given the names UC-1 and UC-2, with IC_{50} values of 11.7 and 44 μM, respectively. Other inhibitors with IC_{50} values higher than 50 μM were determined to have insignificant inhibition potential with EndoU and were not studied further. There seemed to be no correlation between the GLIDE scores and the actual experimental values for percent inhibition and IC_{50} values.

Structure No	CatalogID	Structure No	CatalogID
1	Z56973669	12	Z1455304686
2	Z26321870	13	Z1455356938
3	Z19958244	14	Z1455179836
4	Z336087488	15	Z15671361
5	Z192484250	16	Z2379494531
6	Z595832840	17	Z68839472
7	Z827306036	18	Z2755084966
8	Z190097804	19	Z2607799190
9	Z2055856848	20	Z1870053791
10	Z2060926575	21	Z1603598598
11	Z1443621753	22	Z2835591650

Table 3.2: The Enamine ID names for compounds screened along with the numbers we assigned to each for convenience.

(A) *(B)*

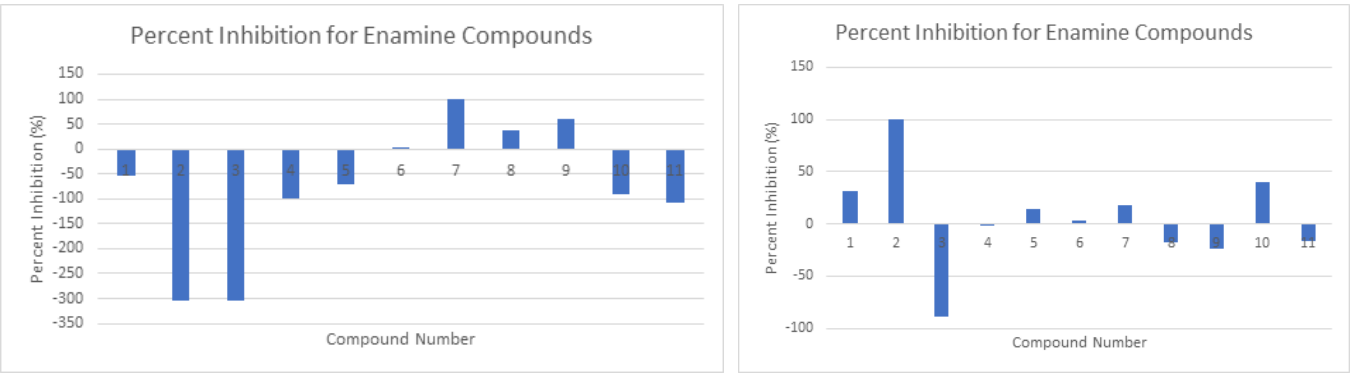

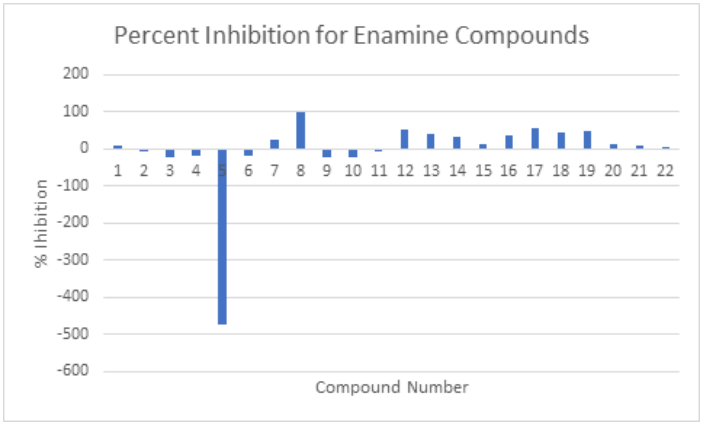

(C)

Figure 3.1: Each compound from Enamine (labeled with corresponding numbers shown in Table 3.2) with the best Glide scores were screened to assess the percentage of inhibition of fluorescent emission as compared with the control (A). The same screen was repeated (B) and then a third time with all 22 compounds (C).

More Enamine compounds that are analogues of UC-1 and UC-2 were assayed to assess the percent inhibition of EndoU. Figure 3.1A shows how some compounds seemed to exhibit full inhibition of EndoU while others seemed to activate the cleavage activity of EndoU. Repeated trials of the assay depicted by Figure 3.1B and C show inconsistent results. In Figure 3.1A, compound 7 (Enamine ID Z827306036) was thought to fully inhibit substrate cleavage by EndoU but has a fraction of the same effect in Figure 3.1B and C, which suggested large random errors in the data.

(A) *(B)*

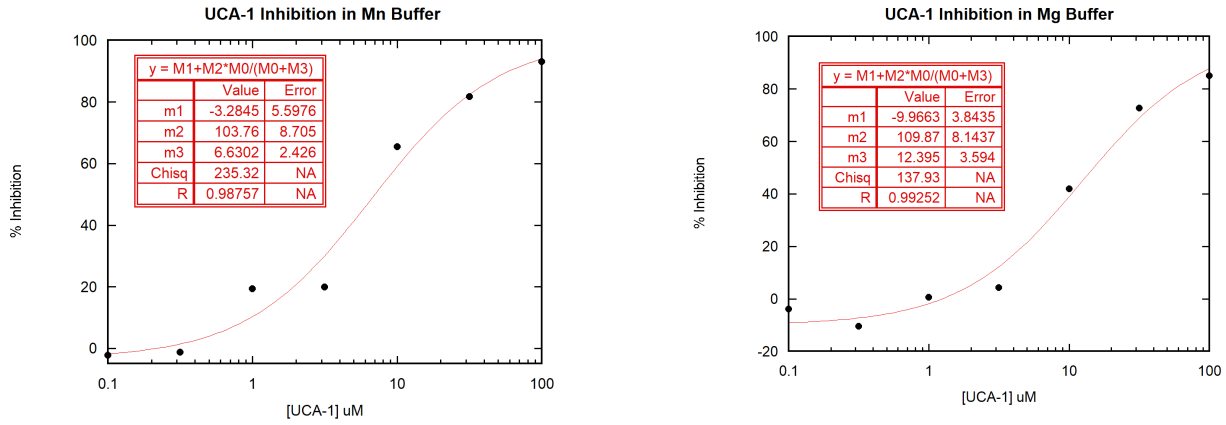

Figure 3.2: Titration curve for UCA-1 in two different divalent ion buffers: manganese (A) and magnesium (B). The "m3" value in each legend represents the IC_{50}.

To test whether the metal was involved in inhibitor binding, one of the promising compounds, UCA-1, was titrated separately with two different reaction buffers, one with manganese as the divalent ion and the other with magnesium. We found an IC_{50} of 6.6 µM in manganese buffer (Figure 3.2A) and 12.4 µM in magnesium buffer (Figure 3.2B). According to this assay, UCA-1 is nearly twice as potent in Mn^{2+} buffer as in Mg^{2+} buffer.

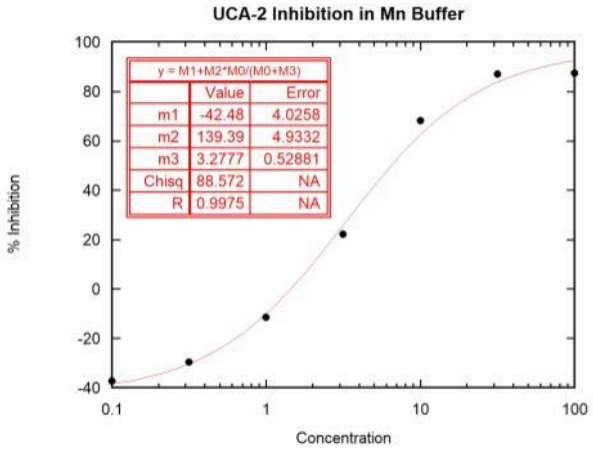

Figure 3.3: Titration curve for UCA-2 in manganese buffer. The "m3" value in the legend represents the IC_{50}

Another of the compounds screened by Dr. Cole that we titrated in buffers with different divalent ions was UCA-2. In the manganese buffer, UCA-2 had an IC_{50} of 3.3 µM (Figure 3.3). The data

from the assay in the magnesium buffer was not fitted because the IC_{50} was over 100 µM which is above our cutoff for a viable inhibitor. It is notable that the inhibition only occurs in the presence of manganese, not magnesium.

(A) *(B)*

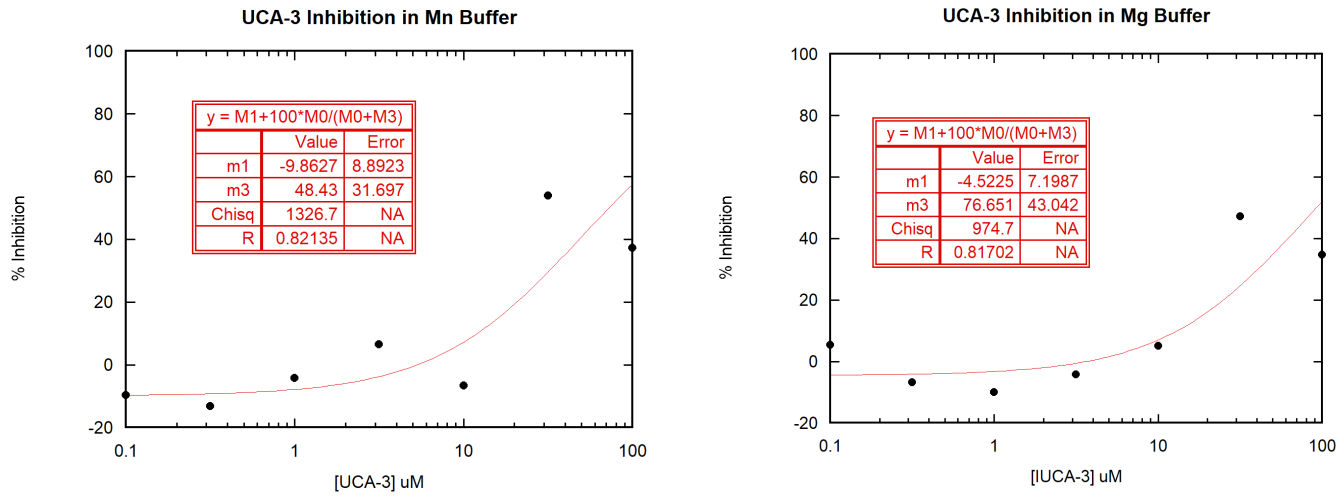

Figure 3.4: Titration curve for UCA-3 in two different divalent ion buffers: manganese (A) and magnesium (B). The m3 corresponds to the IC_{50}.

The next compound from Dr. Cole's screening that we titrated in the two buffers was UCA-3. For this compound, the IC_{50} was 48.4 µM in manganese buffer and 76.6 µM in magnesium buffer (Figure 3.4). These titrations showed low levels of inhibition, so their curves had to be adjusted by artificially setting the maximal % inhibition ("m2") value to 100, despite the fact that neither compound fully inhibited EndoU at the highest concentrations we tested. We also titrated UCA-4 in both buffers but were unable to fit the data as the IC_{50} was over 100 µM in both buffers.

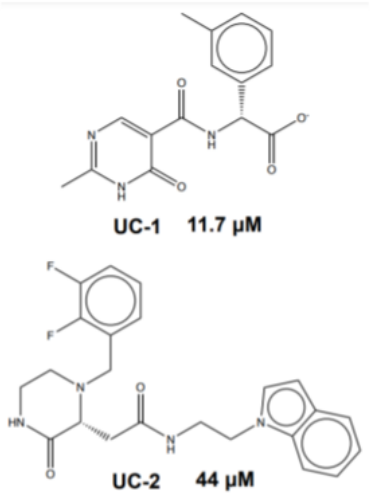

Figure 3.5: Structures and IC_{50} values of compounds from Chembridge screened by Dr. Cole for their inhibition of EndoU.

3. 2 Screening of Chembridge Compounds

We next tested the effects of different divalent cations on the inhibition of EndoU by UC-1 and UC-2. Just as with the Atomwise compounds, each of these compounds were assayed in both manganese and magnesium buffers to test whether the divalent ion affected potency of the inhibition. For the compound UC-1, we observed an IC_{50} of 1.4 µM in the manganese buffer and 39.1 µM in the magnesium buffer (Figure 3.6).

(A)

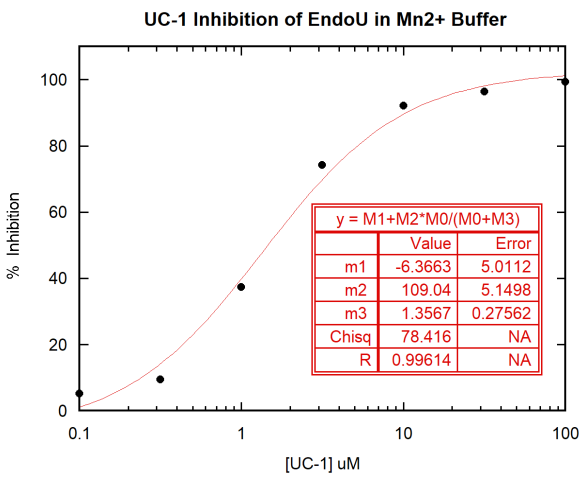

(B)

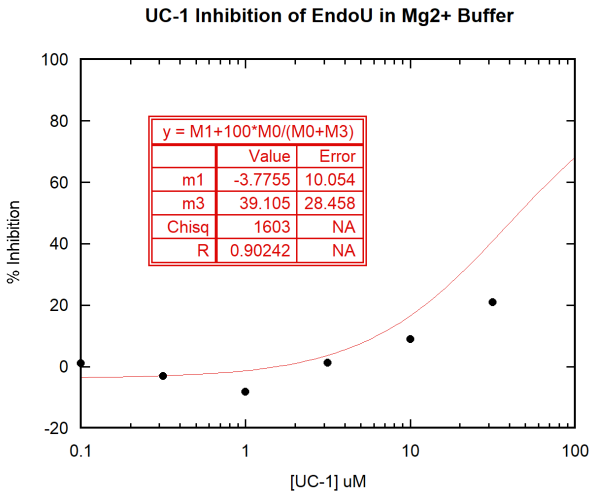

Figure 3.6: Titration curve for UC-1 in two different divalent ion buffers: manganese (A) and magnesium (B). The "m3" value in each legend represents the IC_{50}.

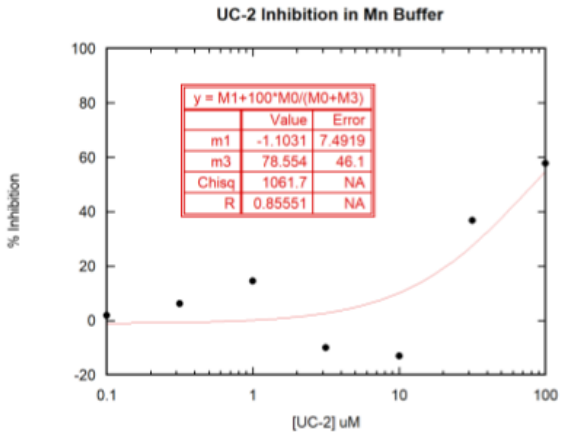

Figure 3.7: Titration curve for UC-2 in manganese buffer. The "m3" value in each legend represents the IC_{50}

For the compound UC-2, we observed an IC_{50} of 78.6 µM in the manganese buffer (Figure 3.7). Just as with the UCA-3 titrations, the equation for this curve had to be adjusted by manually setting the maximum inhibition to 100%. We were unable to fit the data for UC-2 inhibition in the magnesium buffer as the IC_{50} value was over 100 µM.

3.3 Titration of SARS-CoV-1 Inhibitors with EndoU

(A) *(B)*

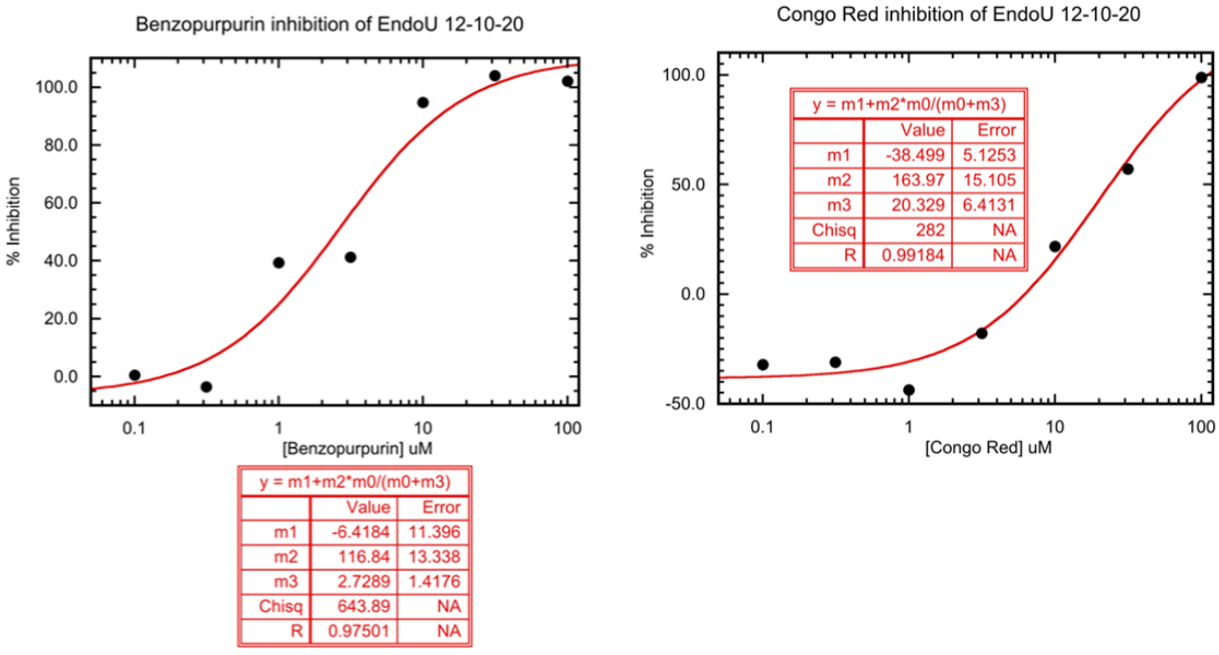

Figure 3.8: Titration curve for compounds Benzopurpurin (A) and Congo Red (B). The "m3" value in each legend represents the IC_{50}.

Benzopurpurin and Congo Red, compounds that are known inhibitors of the nsp15 homolog from SARS-CoV-1 (18), were titrated to test their potency as inhibitors of EndoU from SARS-CoV-2. Benzopurpurin is shown to be a relatively potent inhibitor with an IC_{50} of 2.7 μM, as well as Congo Red with an IC_{50} of 20.2 μM (Figure 3.8).

3.4 Titration of Synthetic Inhibitors

Compound ID	Name	Structure	MW (g/mol)	Docking Scores
JB-001	phenylalanine	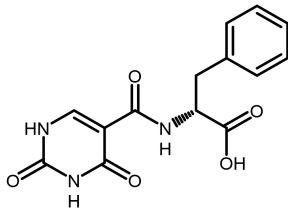	303.9	L: -8.16 D: -8.02
JB-002	ortho-methyl phenyl	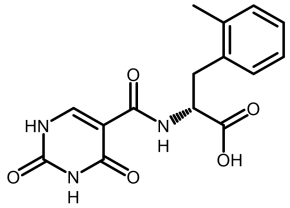	317.1	L: -8.00 D: -7.73
JB-003	lysine	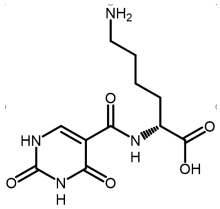	284.11	L: -7.54 D: -8.09

Table 3.3: The ID names, structures, molecular weights, and docking scores for the three compounds synthesized and purified by the Peczuh Lab.

To study the structure-activity relationship of our most potent inhibitors, UC-1, we collaborated with the Peczuh lab to synthesize analogs of this compound, and virtually screened them to assess which changes might have the biggest improvement on inhibition (Table 3.3). Although the docking scores we calculated differ by chirality, the compounds synthesized by the Peczuh

lab were racemic mixtures of both stereoisomers. We then titrated the compounds in two separate trials to evaluate their potency with IC_{50} values.

(A) *(B)*

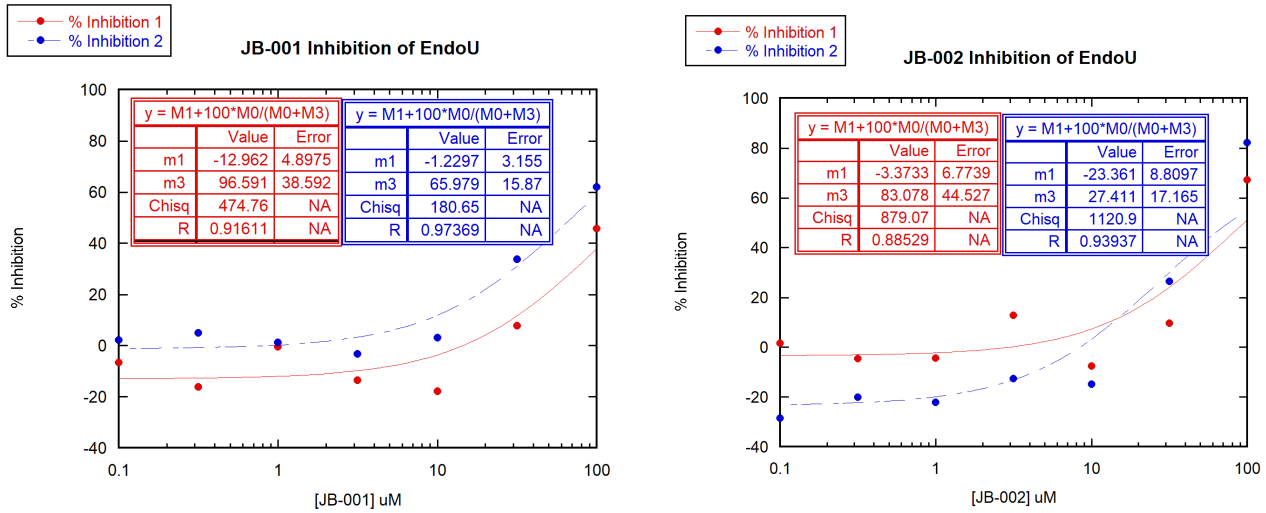

Figure 3.9: Plots of titrations of two of the compounds synthesized by the Peczuh lab, JB-001 and JB-002. The two trials for each compound are superimposed on each graph and labeled in red and blue. The "m3" value in each legend represents the IC_{50}.

For JB-001, we calculated an IC_{50} of 96.6 µM in the first trial and 66.0 µM in the second trial. For JB-002, we calculated an IC_{50} value of 83.1 µM for the first trial and 27.4 µM for the second trial. The data for the titration of JB-003 could not be fit because the IC_{50} was over 100 µM in each trial.

4. Discussion

Inhibitor	IC_{50} (μM) in Mn^{2+} Buffer	IC_{50} (μM) in Mg^{2+} Buffer	Ratio of IC_{50} Mg^{2+}:IC_{50} Mn^{2+}
UCA-1	6.6302	12.395	1.87
UCA-2	3.2777	>100	-
UCA-3	48.43	76.651	1.58
UCA-4	>100	>100	-
UC-1	1.3567	39.105	28.57
UC-2	78.554	>100	-

Table 4.1: A compilation of all IC_{50} values from titrations comparing inhibition using different ion buffers and their ratio.

In this study, I identified no new inhibitors through my screenings of commercially available compounds (Figure 3.1). However, I was able to characterize inhibitors of nsp15 that were previously identified by Dr. Cole. Each of the inhibitors in Table 4.1 were titrated in both manganese and magnesium buffers to test whether the type of ion cofactor present in the buffer affected the ability of the compounds to inhibit the enzyme. Each inhibitor had a lower IC_{50} (exhibiting more potency) in the manganese buffer than the magnesium buffer. For many of the compounds titrated, only a fraction of the compound was needed to inhibit EndoU in the presence of manganese than was needed in the presence of magnesium. For example, UC-1 had an IC_{50} of 1.4 μM in the presence of Mn^{2+} and 39.1 μM in the presence of Mg^{2+} which gives nearly a 30-fold increase in potency of the compound in the manganese buffer (Table 4.1). Previous studies of nsp15 from SARS-CoV-1 suggest that it is a divalent-ion-dependent endoribonuclease which prefers Mn^{2+} as a cofactor over Mg^{2+} (20). The divalent ion cofactor was thought to cause a conformational change in the enzyme that alters it into an active catalytic

state, with Mn^{2+} being significantly more potent than Mg^{2+}. Additional research on the divalent ion dependence of the SARS-CoV-2 nsp15 homolog were unable to identify a metal-binding site in the crystal structure enzyme, but proposed that the metal cofactor could play a role in maintaining substrate conformation during catalysis (5,17). It is believed that nsp15 follows the RNAse mechanism as demonstrated by Figure 4.1 below.

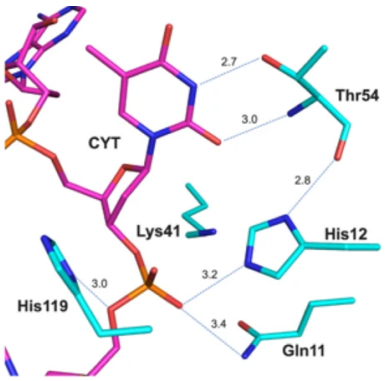

Figure 4.1: Active site of RNAse A is compared with that of Nsp15 in the complex with transition state analog uridine 2',3'-vanadate (from reference (17))

There is no current literature on the effect of the divalent ion on inhibition, but our data suggests that our inhibitors exhibit more potency in the presence of Mn^{2+} than Mg^{2+}. It is unclear where these cofactors bind or interact with the enzyme, but they do seem to somehow influence inhibitor binding. Additional research is needed to solve the structure of the enzyme's interaction with the divalent metal ion to possibly identify the binding site and whether or not it affects the enzyme's interaction with the substrate or inhibitor.

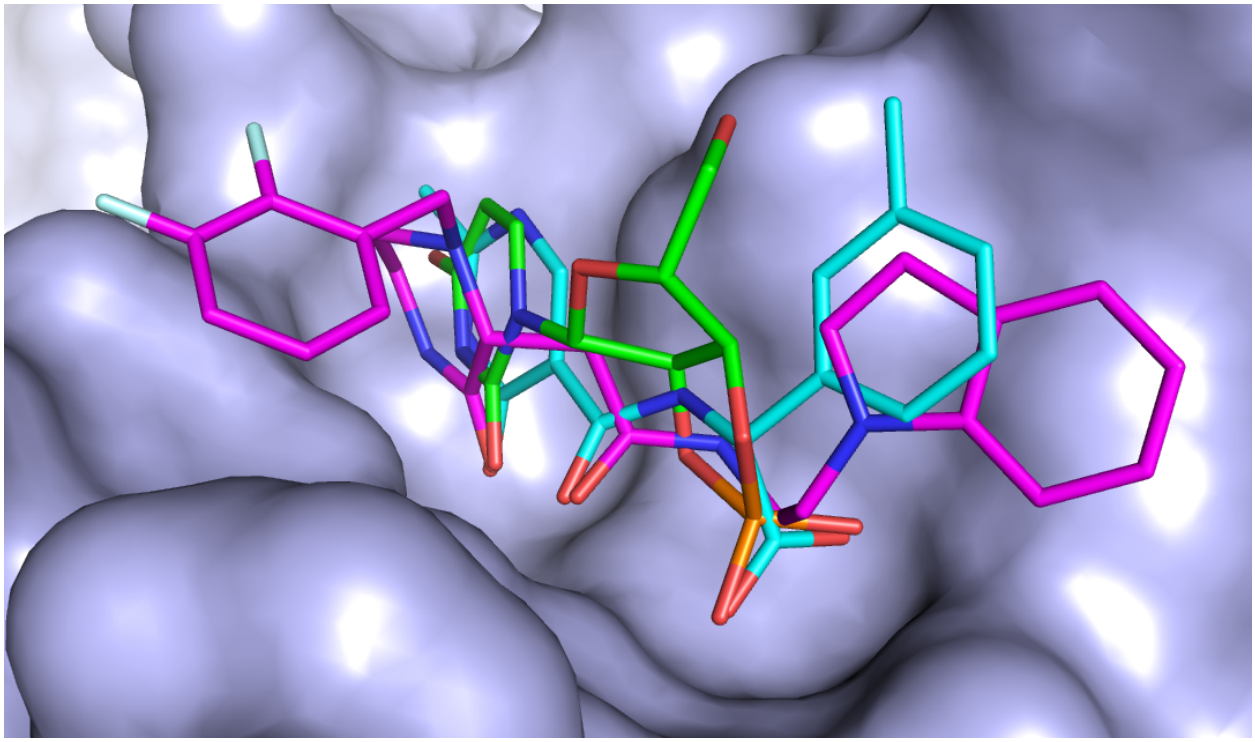

Figure 4.2: Ligand poses from GLIDE. Overlay of 2'-'3-UMP with pyrimidine hits. green, 2'-3'-UMP; cyan, UC-1; purple, UC-2

Additional findings from the study include that previously identified inhibitors of the SARS-CoV-1 nsp15 are also reasonable inhibitors of the SARS-CoV-2 homolog, which was the expected result because their structures are similar. As seen by the docked conformations in Figure 4.2, the structures of UC-1 and UC-2 are remarkably similar to the product analogue, uridine 2'-3'-cyclic monophosphate (2'-3'-UMP) .. The UC-1 analogs synthesized by the Peczuh Lab were not effective inhibitors of EndoU due to their differences in structure from UC-1. More analogs of existing compounds are needed to further investigate the structure-function relationships between inhibitors and EndoU.

References

1. *Origin of SARS-CoV-2*, World Health Organization, 26 Mar. 2020, WHO/2019-nCoV/FAQ/Virus_origin/2020.1.
2. "WHO Coronavirus (COVID-19) Dashboard." World Health Organization, World Health Organization, 28 Sept. 2021, https://covid19.who.int/.
3. De, Priyasha, et al. "Brief Review on Repurposed Drugs and Vaccines for Possible Treatment of COVID-19." *European Journal of Pharmacology*, vol. 898, 2021, p. 173977., https://doi.org/10.1016/j.ejphar.2021.173977.
4. V'kovski, Philip, et al. "Coronavirus Biology and Replication: Implications for SARS-COV-2." *Nature Reviews Microbiology*, vol. 19, no. 3, 2020, pp. 155–170., https://doi.org/10.1038/s41579-020-00468-6.
5. Kim, Youngchang, et al. "Crystal Structure of NSP15 Endoribonuclease NEndoU from SARS‐COV‐2." *Protein Science*, vol. 29, no. 7, 2020, pp. 1596–1605., https://doi.org/10.1002/pro.3873.
6. Deng, Xufang, and Susan C. Baker. "An 'Old' Protein with a New Story: Coronavirus Endoribonuclease Is Important for Evading Host Antiviral Defenses." *Virology*, vol. 517, 2018, pp. 157–163., https://doi.org/10.1016/j.virol.2017.12.024.
7. Deng, Xufang, et al. "Coronavirus Nonstructural Protein 15 Mediates Evasion of Dsrna Sensors and Limits Apoptosis in Macrophages." *Proceedings of the National Academy of Sciences*, vol. 114, no. 21, 2017, https://doi.org/10.1073/pnas.1618310114.
8. Kindler, Eveline, et al. "Early Endonuclease-Mediated Evasion of RNA Sensing Ensures Efficient Coronavirus Replication." *PLOS Pathogens*, vol. 13, no. 2, 2017, https://doi.org/10.1371/journal.ppat.1006195.
9. Hackbart, Matthew, et al. "Coronavirus Endoribonuclease Targets Viral Polyuridine Sequences to Evade Activating Host Sensors." *Proceedings of the National Academy of Sciences*, vol. 117, no. 14, 2020, pp. 8094–8103., https://doi.org/10.1073/pnas.1921485117.
10. Canal, Berta, et al. "Identifying Sars-COV-2 Antiviral Compounds by Screening for Small Molecule Inhibitors of NSP15 Endoribonuclease." *Biochemical Journal*, 478, 2465-2479, 2021, https://doi.org/10.1101/2021.04.07.438811.
11. Stevaert, Annelies, et al. "Betulonic Acid Derivatives Interfering with Human Coronavirus 229e Replication via the NSP15 Endoribonuclease." *Journal of Medicinal Chemistry*, vol. 64, no. 9, 2021, pp. 5632–5644., https://doi.org/10.1021/acs.jmedchem.0c02124.
12. Hayn, Manuel, et al. "Systematic Functional Analysis of SARS-COV-2 Proteins Uncovers Viral Innate Immune Antagonists and Remaining Vulnerabilities." *Cell Reports*, vol. 35, no. 7, 2021, p. 109126., https://doi.org/10.1016/j.celrep.2021.109126.

13. Imran, Mohd., et al. “Discovery, Development, and Patent Trends on Molnupiravir: A Prospective Oral Treatment for Covid-19.” *Molecules*, vol. 26, no. 19, 2021, p. 5795., https://doi.org/10.3390/molecules26195795.
14. Frieman, Matthew, et al. “Severe Acute Respiratory Syndrome Coronavirus Papain-like Protease Ubiquitin-like Domain and Catalytic Domain Regulate Antagonism of IRF3 and NF-KB Signaling.” *Journal of Virology*, vol. 83, no. 13, 2009, pp. 6689–6705., https://doi.org/10.1128/jvi.02220-08.
15. Frazier, Meredith N., et al. “Characterization of sars2 NSP15 Nuclease Activity Reveals It’s Mad about U.” *Nucleic Acids Research*, vol. 49, 2021, pp. 10136–10149., https://doi.org/10.1101/2021.06.01.446181.
16. Perry, Jason K., et al. “An Atomistic Model of the Coronavirus Replication-Transcription Complex as a Hexamer Assembled around NSP15.” *Journal of Biological Chemistry*, vol. 297, no. 4, Oct. 2021, https://doi.org/10.1101/2021.06.08.447516.
17. Kim, Youngchang, et al. “Tipiracil Binds to Uridine Site and Inhibits NSP15 Endoribonuclease Nendou from SARS-COV-2.” *Communications Biology*, vol. 4, no. 1, 2021, https://doi.org/10.1038/s42003-021-01735-9.
18. Ortiz-Alcantara, J, et al. “Small Molecule Inhibitors of the SARS-COV NSP15 Endoribonuclease.” *Virus Adaptation and Treatment*, no. 2, 3 Sept. 2010, pp. 125–133., https://doi.org/10.2147/vaat.s12733.
19. RCSB Protein Data Bank. “6VWW.” *Crystal Structure of NSP15 Endoribonuclease from SARS CoV-2*., 4 Mar. 2020, https://www.rcsb.org/3d-view/6VWW/1.
20. Bhardwaj, Kanchan, et al. “The Severe Acute Respiratory Syndrome Coronavirus NSP15 Protein Is an Endoribonuclease That Prefers Manganese as a Cofactor.” *Journal of Virology*, vol. 78, no. 22, 2004, pp. 12218–12224., https://doi.org/10.1128/jvi.78.22.12218-12224.2004.